34th Annual International Conference of the IEEE EMBS
San Diego, California USA, 28 August - 1 September, 2012

Three-Way FMRI-DTI-Methylation Data Fusion Based on mCCA+jICA and Its Application to Schizophrenia

Jing Sui*, *Member IEEE,* Hao He, Jingyu Liu, *Member IEEE*, Qingbao Yu, Tülay Adali, *Fellow IEEE*, Godfrey D Pearlson and Vince D Calhoun, *Senior Member IEEE*

Abstract — **Multi-modal fusion is an effective approach in biomedical imaging which combines multiple data types in a joint analysis and overcomes the problem that each modality provides a limited view of the brain. In this paper, we propose an exploratory fusion model, we term "mCCA+jICA", by combining two multivariate approaches: multi-set canonical correlation analysis (mCCA) and joint independent component analysis (jICA). This model can freely combine multiple, disparate data sets and explore their joint information in an accurate and effective manner, so that high decomposition accuracy and valid modal links can be achieved simultaneously. We compared mCCA+jICA with its alternatives in simulation and applied it to real fMRI-DTI-methylation data fusion, to identify brain abnormalities in schizophrenia. The results replicate previous reports and add to our understanding of the neural correlates of schizophrenia, and suggest more generally a promising approach to identify potential brain illness biomarkers.**

I. Introduction

Recently, collecting multiple types of data from the same individual using various techniques including MRI, DTI, EEG and genotyping *etc*., has become common practice. Each brain imaging technique provides a different view of brain function or structure, while genetic variation data can inform on human risk and treatment response. It is increasing clear that multimodal fusion may reveal hidden relationships and unify disparate neuroimaging findings [1]. For example, combining genetic and fMRI data achieves better classification accuracy than using either alone, indicating that genetic and brain function represent different, but partially complementary aspects[2]. Therefore, examination of cross-information among data types may uncover potentially important variations which are only partially detected by each modality.

Existing multivariate fusion methods have different optimization priorities and limitations: Some enable common as well as distinct levels of connection among modalities, such as multi-set canonical correlation analysis (mCCA)[3] and partial least squares (PLS)[4, 5] approaches, but their separated sources may not be sufficiently spatially sparse (e.g., the brain maps of several components may look similar when the correlation coefficients of the canonical variables are insufficiently distinct). Some do well in spatial decomposition, such as joint ICA (jICA)[1] and linked ICA[6], but only allow a common mixing matrix. We aim to solve the above issues by proposing a model that enables both flexible linkages and high decomposition accuracy for multiple brain imaging and genetic data sets, such a fusion strategy is shown in Figure 1. This exploratory model will be compared qualitatively with its alternatives: jICA and mCCA.

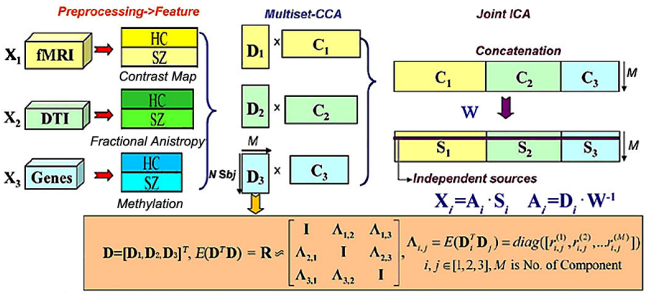

Figure 1. Three way fusion strategy of "mCCA+jICA"

II. Method

We assume that the multimodal dataset $\mathbf{X}_k$, is a linear mixture of M_k sources given by $\mathbf{S}_k$, mixed with a nonsingular mixing matrix $\mathbf{A}_k$ for each, k denotes modality.

$$\mathbf{X}_k = \mathbf{A}_k \mathbf{S}_k \qquad k = 1, 2,..n \qquad (1)$$

where $\mathbf{X}_k$ is a subjects-by-voxels feature matrix (we use voxels for our description but these could also be, *e.g.*, time points or genes). The sources $\mathbf{S}_k$, are distinct within each dataset, while the columns of $\mathbf{A}_i$ and $\mathbf{A}_j$ have higher correlation only on their corresponding indices, $i, j \in \{1, 2..n\}$ $i \neq j$ are modality number. Given that there are N subjects, typically, the number of voxels L in $\mathbf{X}_k$ is much larger than N. Due to the high dimensionality and high noise levels in the brain imaging data, order selection is critical to avoid over fitting the data. Using the improved minimum description length(MDL) criterion as in[7], the number of independent components M_k are estimated for each modality and we set the final component number for joint ICA as $M = \max(M_1, M_2 ... M_n)$.

Dimension reduction is then performed on $\mathbf{X}_k$ using singular value decomposition, a scheme where small singular values of the matrix are treated as noise/redundancy are discarded, given

$$\mathbf{Y}_k = \mathbf{X}_k \mathbf{E}_k \qquad k = 1, 2..n \qquad (2)$$

where $\mathbf{Y}_k$ is in size of $N \times M$ and $\mathbf{E}_k$ contains eigenvectors corresponding to significant (higher) eigenvalues.

*Resrach supported by NIH.

Jing Sui is with the Mind Research Network, Albuquerque, NM, 87106 (corresponding author phone: 505-272-1509 e-mail: kittysj@gmail.com).

Hao He, Qingbao Yu, Jingyu Liu and Vince D Calhoun are with the Mind Research Network and Dept. of ECE, University of New Mexico, Albuquerque, NM, 87106. (vcalhoun@unm.edu).

Tülay Adali is with Dept. of CSEE, University of Maryland, Baltimore County, Baltimore, MD, 21250. (adali@umbc.edu)

Godfrey D Pearlson is with Olin Neuropsychiatry Research Center, Hartford, CT and Depts. of Psychiatry and Neurobiology, Yale University, New Haven, CT, 06519. (godfrey.pearlson@yale.edu).

Multi-set CCA[8] is thus performed on $\mathbf{Y}_k$, generating the canonical variants (CV) $\mathbf{D}_k^T = \mathbf{w}_k \mathbf{Y}_k^T$ by maximizing the sum of squares of all correlation values in the corresponding columns of $\mathbf{D}_k$ so that

$$E\{\mathbf{D}_k^T \mathbf{D}_k\} = \mathbf{I} \;;\; E\{\mathbf{D}_i^T \mathbf{D}_j\} \approx diag(r_{ij}^1, r_{ij}^2 ... r_{ij}^M) \quad (3)$$

where $k, i, j \in \{1, 2...n\}, i \neq j$. Based on the linear mixture model, we simultaneously obtain the associated components $\mathbf{C}_k$ via $\mathbf{X}_k$=$\mathbf{D}_k$ $\mathbf{C}_k$. However, the performance of mCCA for blind source separation (BSS) may suffer when $r_{ij}^1, r_{ij}^2 ... r_{ij}^M$ are very close in values, which might occur in applications using real brain data, since the multimodal connections among components usually are not high and could be similar in value[9]. Therefore, $\mathbf{C}_k$ will typically be a set of sources that do not completely independent.

Joint ICA is then implemented on the concatenated maps[$\mathbf{C}_1$,$\mathbf{C}_2$...$\mathbf{C}_n$], to maximize independence among joint components by reducing their second and higher order statistical dependencies, as in equation (4). ICA as a central tool for BSS has been studied extensively and we utilized Infomax[10] in our work due to its high stability.

$$[\mathbf{S}_1, \mathbf{S}_2 .. \mathbf{S}_n] = \mathbf{W} \cdot [\mathbf{C}_1, \mathbf{C}_2 .. \mathbf{C}_n] \quad (4)$$

Finally, n sets of independent components $\mathbf{S}_k$ are extracted (n=3 in our case), with their corresponding mixing matrices $\mathbf{A}_k$ linked via correlation. The proposed scheme "mCCA+jICA" can be summarized as shown in Figure 1.

$$\mathbf{X}_k = (\mathbf{D}_k \cdot \mathbf{W}^{-1}) \cdot \mathbf{S}_k, \quad \mathbf{A}_k = \mathbf{D}_k \cdot \mathbf{W}^{-1} \quad (5)$$

III. Simulation

We next investigate the joint BSS performance of mCCA+jICA on simulated data and compare it to that of joint ICA and mCCA. 3 modalities with different data length were simulated; each included 8 sources, resulting in true sources $\mathbf{S}_1$ (in size of 8×65536), $\mathbf{S}_2$ (in size of 8×2000) and $\mathbf{S}_3$(in size of 8*10000). The mixing matrices of each modality: $\mathbf{A}_1$, $\mathbf{A}_2$ and $\mathbf{A}_3$ (in size of 100×8), had diverse correlations between their corresponding columns, as the true connection shown in Figure 2(c). 100 noisy mixed images were generated for each modality under each of the 11 noisy conditions via $\mathbf{X}_k = \mathbf{I}_k + \mathbf{N}_k = \mathbf{A}_k \mathbf{S}_k + \mathbf{N}_k$, k=1,2,3; where $\mathbf{I}_k$ is pure signal mixture and $\mathbf{N}_k$ is random Gaussian noise. The corresponding mean peak signal-to-noise ratios (PSNR) are in range of [-1 20] dB. Typical PSNR value for the acceptable image quality is about 30 dB; the lower the value, the more degraded the image[11]. Three joint BSS models: jICA, mCCA and mCCA+jICA were implemented on $\mathbf{X}_k$ respectively under every PSNR for 10 runs. The decomposed components were paired with the true sources via cross-correlation automatically within each feature. We adopted 3 metrics to estimate the joint BSS performance:

1) Estimation accuracy of sources $\mathbf{S}_k$;
2) Estimation accuracy of mixing matrices $\mathbf{A}_k$
3) Mean square error of the modal links ($\mathbf{A}_i$-$\mathbf{A}_j$ correlation) compared to ground truth.

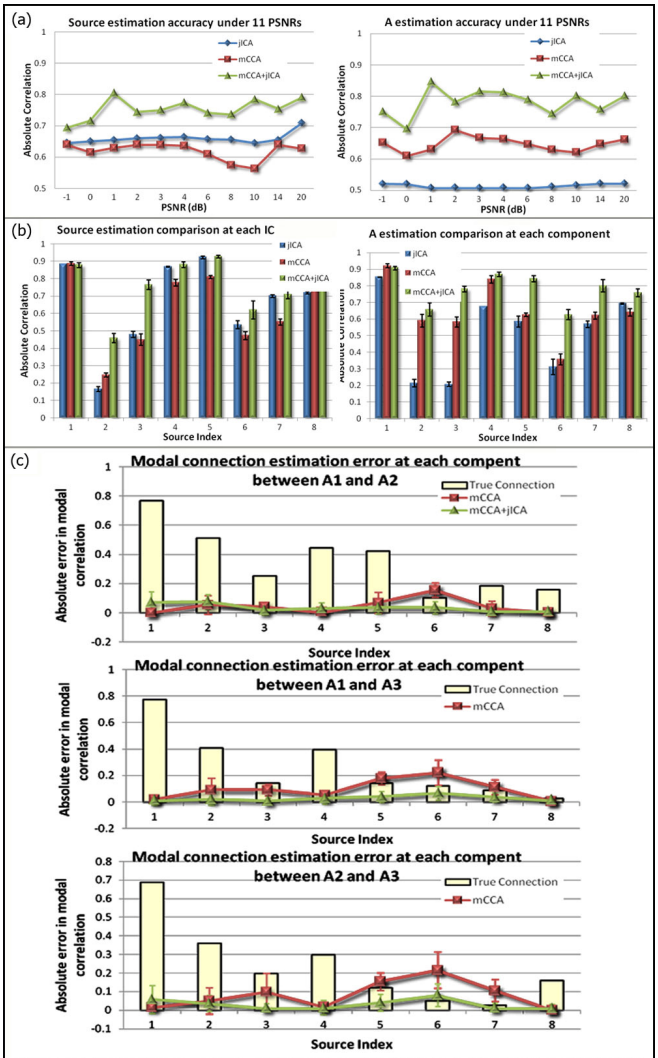

Figure 2 | Comparison of jICA, mCCA and mCCA+jICA in a simulated 3-way fusion Note the noise level is measured by the peak signal to noise ratio (PSNR) and the acceptable image quality is usually with PSNR>=30dB

Figure 2 compared the first two performance metrics in different noisy conditions (a) and source distributions (b). It is evident that mCCA+jICA was quite robust to noise, and its BSS performance was consistently the best in all noise conditions. Consequently, joint ICA was the second best in source estimation and mCCA was the second best in mixing matrix estimation; Note that when PSNR=-1dB, *i.e.*, noise is bigger than signal, all three methods can still have the estimation accuracy higher than 0.5.

Figure 2(c) compared the modal-connection estimation, where the true $\mathbf{A}_1$-$\mathbf{A}_2$, $\mathbf{A}_1$-$\mathbf{A}_3$ and $\mathbf{A}_2$-$\mathbf{A}_3$ correlations were given by yellow bars for every source, while the mean square errors and the standard derivations of the link estimation were plotted in red for mCCA and in green for mCCA+jICA. Note that both high (0.79) and low (0.07) correlation values exist in modal connections, representing shared or distinct factors among modalities. mCCA+jICA again overperformed mCCA, especially for sources whose have low $\mathbf{A}_i$-$\mathbf{A}_j$ correlation values that are close to many others, *e.g.* the $\mathbf{A}_1$-$\mathbf{A}_2$ and $\mathbf{A}_1$-$\mathbf{A}_3$ correlation of source 6.

IV. Real Human Data

Next, mCCA+jICA was applied to real DTI, fMRI (auditory sensorimotor [SM] task[12]) and methylation data collected from 80 healthy controls (HC) and 62 patients with schizophrenia (SZ) derived from four sites of the *MIND Clinical Imaging Consortium* (MCIC) study. Table 1 lists the demographic information for all subjects. WRAT III is a very brief screening measure for achievement.

Table 1. Subject Demographic Information .

	Number (sex)	*Age*	*WRAT III*	*Ethnicity*
HC	80 (29 female)	32.4±11.1	51±4.2	66 white
SZ	62 (16 female)	33.5±10.8	46±6.8	49 white
***p* value**	0.45	0.55	5e-7	0.55

Our goal was to identify the aberrant brain regions or genetic features in schizophrenia and to examine whether these factors share connections among brain function, structure and genetic methylation. Based on the theory described in the Methods section, M=11 was estimated as the model order.

A. Preprocessing

FMRI data were preprocessed using SPM5 software (http://www.fil.ion.ucl.ac.uk/spm/software/spm5/), resulting in 53×63×46 voxels. A GLM analysis consisted of a univariate multiple regression of each voxel's time course with an experimental design matrix was used to find task-associated brain regions. We utilized the subtraction of tapping beta-weight map with experimental baseline to represent the tapping effect for the SM task.

DTI data were preprocessed by FMRIB Software Library (FSL; www.fmrib.ox.ac.uk/fsl) consists of the following steps: 1) Quality check 2) Motion and eddy current correction 3) Adjusting diffusion gradient direction and 4) Feature extraction, to calculate the diffusion tensor and fractional anisotropy (FA) maps, which were then smoothed and resized to a final 53×63×46 matrix for each subject.

The raw methylation data have 27.5K locus in which the measurement error was first corrected by selecting locus that only has standard derivation >0.05, thus reducing the effective length to 1266 locus (contain 1108 unique genes). Then the gender effect was corrected using principal component analysis (PCA) by removing the PCs that show strong correction with sex.

After feature extraction, the 3D brain image of each subject was reshaped into a one-dimensional non-zero vector and stacked one by one, forming a matrix with dimensions of 142×[number of voxels] for fMRI or DTI. The site effect was corrected by making the mean of data from 4 sites equal. The methylation data matrix (142×1266) had no significant site effect, but a strong batch effect that was also corrected by making the mean of data from all batches equal. Then 3 feature matrices were normalized to have the same average sum-of-squares (computed across all subjects and all voxels/loci for each modality). The normalization was needed because all modalities had different ranges. Thus, following normalization, the relative scaling (a normalization factor) within a given data type was preserved, but the units between data types were the same (in a least-squares sense). After normalization, the data were processed via the pipeline shown in Figure 1, *i.e.*, dimension reduction-> mCCA-> jICA-> component analysis. Note that the mCCA+jICA approach does not increase the computational load appreciably. It only cost minutes to analyze hundreds of subjects, however it integrates merits of both joint ICA and multi-set CCA.

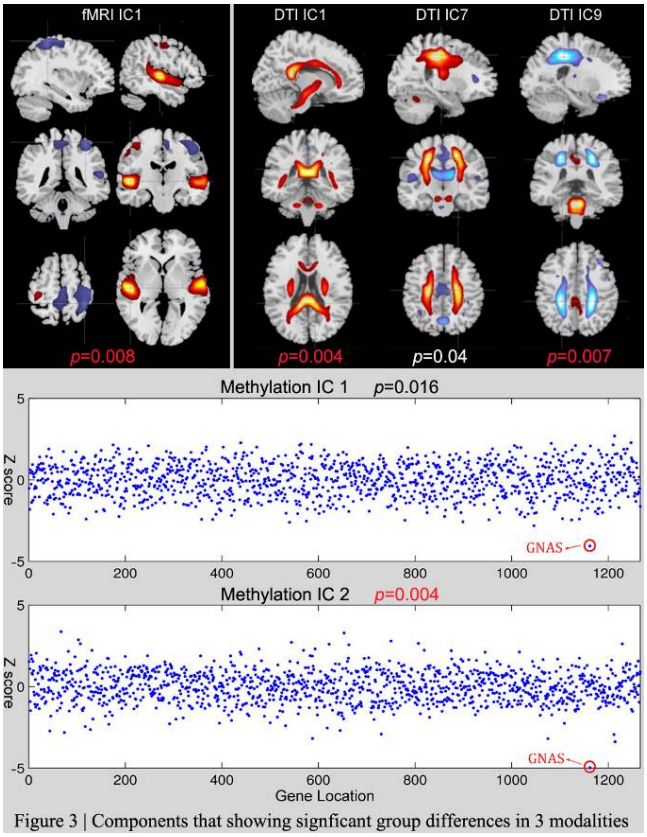

Figure 3 | Components that showing signficant group differences in 3 modalities

B. Results of Group Differences

Two sample t-tests were performed for fMRI and DTI on its mixing coefficients between controls and schizophrenia. As methylation data are strongly affected by aging and may be affected by race, we employed an ANOVA of 3 factors (group, age and race) on the methylation loading parameters and selected those components with significant group effects. Results are shown in Figure 3, with p values displayed within the component plots. The reported p values surviving false discovery rate correction for multiple comparisons are shown in red. One joint component (IC 1) and three modality-specific components(DTI_IC7, DTI_IC9 and Methl_IC2) were identified as group-discriminating ICs, thus our method showed more flexibilities than joint ICA in detecting group differences in loadings.

FMRI_IC1 depicts a set of well known regions previously implicated in schizophrenia during a SM task, including superior temporal gyrus (STG) and motor cortex, consistent with the fact that this is an auditory task requiring subjects to push buttons. STG plays a prominent role in schizophrenia, e.g. It has been identified as the most group-discriminating region for controls versus schizophrenia

patients in auditory tasks such as the sensorimotor paradigm[13] and its dysfunction has been related to the auditory hallucinations that are common in schizophrenia [14].In addition, motor activation deficits in schizophrenia are frequently detected in fMRI studies[15].

DTI_IC1 identified large regions in the cortico-spinal tract (CST) and superior longitudinal fasciculus (SLF), especially SLFt (the parts of SLF from temporal lobe), which originate from the caudal STG, pass along with the SLF bundle and terminate in the prefrontal cortex. This suggests that the "linked" (joint) brain components correspond to FA changes in known tracts and functional changes in distant regions connected to those tracts.

DTI_IC 7 and DTI_IC 9 detect other discriminative regions in tracts of anterior thalamic radiation (ATR) and inferior fronto-occipital fasciculus (IFO). This finding was consistent with several reports of DTI abnormalities in SZ [16], suggesting that disruptions in white matter connectivity may contribute to coordinated brain dysfunction, especially in the frontal lobe, which frequently is thought of as "disconnected" from other brain regions in schizophrenia[17].

For methylation data, one gene in the same location of IC1 and IC2 had the highest Z score, that is, GNAS (G protein alpha subunit) located at 20q13.3. Programmed cell death and alterations in intracellular G-protein signaling may be involved in the pathophysiology of schizophrenia. The G-alpha subunit of heterotrimeric G-proteins, encoded by the gene GNAS, may play a role in both of these processes[18] and was associated with schizophrenia in an Italian population sample[19], suggesting an underlying association between the methylation factor and the brain.

V. Conclusion

A chief purpose of multimodal fusion is to access the joint information provided by different data types, which in turn can be useful for identifying dysfunctional processes implicated in brain disorders. In this paper, we extended our previous two-way "mCCA+jICA" model[9] to multi-way fusion, which in simulation was verified as able to achieve higher decomposition accuracy and to identify valid links between modalities. In a real-world fusion application, we highlighted data from brain function, structure and genetics. We identified both modal-common and modal-specific group-discriminating aspects that verified the abnormalities in schizophrenia and replicated previous findings. Such observations add to our understanding of the neural correlates of schizophrenia. The proposed model promises a widespread utilization in the neuroimaging community and may be used to identify potential brain illness biomarkers.

Acknowledgment

This work was supported by the NIH R01EB006841 and R01EB005846 (to Calhoun VD), and R01MH074797 (to Pearlson GD), and the NSF grant 1017718(to Adali T).

References

[1] V.D. Calhoun, T. Adali, N.R. Giuliani, J.J. Pekar, K.A. Kiehl, and G.D. Pearlson, "Method for multimodal analysis of independent source differences in schizophrenia: combining gray matter structural and auditory oddball functional data," *Hum Brain Mapp*, vol. 27, (no. 1), pp. 47-62, Jan 2006.

[2] H. Yang, J. Liu, J. Sui, G.D. Pearlson, and V.D. Calhoun, "A Hybrid Machine Learning Method for Fusing fMRI and Genetic Data: Combining both Improves Classification of Schizophrenia," *Front Hum Neurosci*, vol. 4, pp. 192, 2010.

[3] N.M. Correa, T. Eichele, T. Adali, Y.O. Li, and V.D. Calhoun, "Multi-set canonical correlation analysis for the fusion of concurrent single trial ERP and functional MRI," *NeuroImage*, Jan 25 2010.

[4] K. Chen, E.M. Reiman, Z. Huan, R.J. Caselli, D. Bandy, N. Ayutyanont, and G.E. Alexander, "Linking functional and structural brain images with multivariate network analyses: a novel application of the partial least square method," *NeuroImage*, vol. 47, (no. 2), pp. 602-10, 2009.

[5] F.H. Lin, A.R. McIntosh, J.A. Agnew, G.F. Eden, T.A. Zeffiro, and J.W. Belliveau, "Multivariate analysis of neuronal interactions in the generalized partial least squares framework: simulations and empirical studies," *NeuroImage*, vol. 20, (no. 2), pp. 625-42, Oct 2003.

[6] A.R. Groves, C.F. Beckmann, S.M. Smith, and M.W. Woolrich, "Linked independent component analysis for multimodal data fusion," *NeuroImage*, vol. 54, (no. 3), pp. 2198-2217, Oct 4 2011.

[7] Y.O. Li, T. Adali, and V.D. Calhoun, "Estimating the number of independent components for functional magnetic resonance imaging data," *Hum Brain Mapp*, vol. 28, (no. 11), pp. 1251-66, Nov 2007.

[8] Y.O. Li, T. Adali, W. Wang, and V.D. Calhoun, "Joint Blind Source Separation by Multi-set Canonical Correlation Analysis," *IEEE Trans Signal Process*, vol. 57, (no. 10), pp. 3918-3929, Oct 1 2009.

[9] J. Sui, G. Pearlson, A. Caprihan, T. Adali, K.A. Kiehl, J. Liu, J. Yamamoto, and V.D. Calhoun, "Discriminating schizophrenia and bipolar disorder by fusing fMRI and DTI in a multimodal CCA+ joint ICA model," *NeuroImage*, vol. 57, (no. 3), pp. 839-55, Aug 1 2011.

[10] A.J. Bell and T.J. Sejnowski, "An information-maximization approach to blind separation and blind deconvolution," *Neural Comput*, vol. 7, (no. 6), pp. 1129-59, Nov 1995.

[11] N. Thomos, N.V. Boulgouris, and M.G. Strintzis, "Optimized Transmission of JPEG2000 Streams Over Wireless Channels," *IEEE Trans Image Process*, vol. 15, (no. 1), 2006.

[12] J. Sui, T. Adali, G.D. Pearlson, and V.D. Calhoun, "An ICA-based method for the identification of optimal FMRI features and components using combined group-discriminative techniques," *NeuroImage*, vol. 46, (no. 1), pp. 73-86, May 15 2009.

[13] O. Demirci, V.P. Clark, V.A. Magnotta, N.C. Andreasen, J. Lauriello, K.A. Kiehl, G.D. Pearlson, and D.C. Calhoun, "A Review of Challenges in the use of fMRI for Disease Classification / Characterization and A Projection Pursuit Application from Multi-site fMRI Schizophrenia Study," *Brain Imaging and Behavior*, vol. 2, (no. 3), pp. 207-226, 2008.

[14] V.D. Calhoun, K.A. Kiehl, P.F. Liddle, and G.D. Pearlson, "Aberrant localization of synchronous hemodynamic activity in auditory cortex reliably characterizes schizophrenia," *Biological psychiatry*, vol. 55, (no. 8), pp. 842-9, Apr 15 2004.

[15] J. Schroder, M. Essig, K. Baudendistel, T. Jahn, I. Gerdsen, A. Stockert, L.R. Schad, and M.V. Knopp, "Motor dysfunction and sensorimotor cortex activation changes in schizophrenia: A study with functional magnetic resonance imaging," *NeuroImage*, vol. 9, (no. 1), pp. 81-7, Jan 1999.

[16] R.G. Schlosser, I. Nenadic, G. Wagner, D. Gullmar, K. von Consbruch, S. Kohler, C.C. Schultz, K. Koch, C. Fitzek, P.M. Matthews, J.R. Reichenbach, and H. Sauer, "White matter abnormalities and brain activation in schizophrenia: a combined DTI and fMRI study," *Schizophrenia research*, vol. 89, (no. 1-3), pp. 1-11, Jan 2007.

[17] L.M. Williams, P. Das, A.W. Harris, B.B. Liddell, M.J. Brammer, G. Olivieri, D. Skerrett, M.L. Phillips, A.S. David, A. Peduto, and E. Gordon, "Dysregulation of arousal and amygdala-prefrontal systems in paranoid schizophrenia," *The American journal of psychiatry*, vol. 161, (no. 3), pp. 480-9, Mar 2004.

[18] S.W. Robinson and M.G. Caron, "Selective inhibition of adenylyl cyclase type V by the dopamine D3 receptor," *Mol Pharmacol*, vol. 52, (no. 3), pp. 508-14, Sep 1997.

[19] P. Minoretti, P. Politi, E. Coen, C. Di Vito, M. Bertona, M. Bianchi, and E. Emanuele, "The T393C polymorphism of the GNAS1 gene is associated with deficit schizophrenia in an Italian population sample," *Neurosci Lett*, vol. 397, (no. 1-2), pp. 159-63, Apr 10-17 2006.